Synthesis and Characteristics of 316L Porous Biomaterial using the Pore Formation Technique Aided by Polyurethane Sponge

Muh Amin[1,*] Muhammad Subri[2] Bagus Irawan Widyawardhana[3] Solechan Solechan[4] Adit Bagos Suwantoro[5]
[1,2,3,4,5]Universitas Muhamamdiyah Semarang, Semarang, Central Java 50273, Indonesia
amin@unimus.ac.id

Abstract. The ability of porous biomedical implants to stimulate bone tissue formation has been shown to improve biocompatibility and osseointegration. Since the modulus of elasticity of human bone and implant material differs, porous implants may also provide less protection against stress. This study looked into how porosity control was achieved in AISI 316L bone implant material using PU sponge as the foaming agent. A duplicate template for pore production is used in the suggested method, which is PU sponge media. By combining distilled water with 1% weight tapioca flour to create a green body, PU sponges with porosities of 20, 25, 30, and 35 PPI are impregnated with AISI 316L metal slurry. By measuring the density of PU sponge throughout the creation of green bodies, porosity control was accomplished. Using an optical microscope, the development of the porous AISI 316L's physical and microstructural characteristics was examined. Using an optical microscope at a specific magnification, the powder necking phenomenon was seen. The findings indicate that when the density of PU sponge increases, sample porosity increases as well. Nonetheless, the porosity of the AISI 316L biomaterial decreases as the sintering temperature rises. As the sintering temperature and PU sponge density increase, the sample keeps getting smaller. When creating porous materials for orthopedic implants, the study's findings can be consulted.

Keywords: Biomaterial, Implant, Metal Foam, Polyurethane, Porous Material, Stainless Steel.

1. Introduction

Due to its great biocompatibility (Pathote et al., 2023), effective corrosion resistance for orthopedics (Pathote et al., 2022), and high specific strength (Ravichander et al., 2023), the metallic biomaterial AISI 316L has been acknowledged as an excellent material for bone, dental, and orthopedic implants. But as Table 1 illustrates, the Young's modulus of AISI 316L metal is ~193 GPa, which is less than that of bone. This mismatch in Young's modulus between the implant and bone might cause protective stress, which can lead to implant

I. Yustar Afif and R. Nindyo Sumarno (eds.), *Proceedings of the 2nd Lawang Sewu International Symposium on Engineering and Applied Sciences (LEWIS-EAS 2023)*, Advances in Engineering Research 234,
https://doi.org/10.2991/978-94-6463-480-8_10

failure (Essa et al., 2018). As per Čapek et al. (2016), a low modulus porous material was therefore required to avoid stress-shielding effects.

Equalizing the elastic modulus of implants is one way to address the disparity between their mechanical characteristics and those of human bones. Making it a porous material is one way to accomplish that (Du et al., 2021). The benefits of porous implants include improved bone-graft bonding, faster tissue growth, and easier medication and bodily fluid transmission via channels (Singh et al., 2021). The link between the implant and the bone can be strengthened by producing porous implant material. Additionally, it permits the growth of bodily tissues, which improves metals' osseointegration and biocompatibility in biomedical applications (Bandyopadhyay et al., 2023).

Anisotropic, multiphase, and heterogeneous properties are seen in human bones. The human skeleton is divided into two halves. Čapek et al. (2016) refer to the cortical bone as one portion and the trabecular bone as the other. Because it lines the outside of the trabecular bone, the cortical bone acts as a shield for the trabecular bone. Accordingly, cortical bone must possess a higher mechanical strength than trabecular bone (Du et al., 2021). Table 1 displays the traits of the two different kinds of bones.

The biomaterial AISI 316L was employed in this study. Using tapioca flour as a pore medium and a PU sponge, the porous material was modified. Using powder metallurgy, the different levels of porosity that are obtained are controlled. Tapioca flour functions as a binder and an agent that generates controllable micropores.

Table 1. Characteristics of human bones

TYPE		CORTICAL BONE		TRABECULAR BONE	
	Loading direction	Ultimate strength/MPa	Elastic modulus/GPa	Ultimate strength/MPa	Elastic modulus/GPa
Compressive mechanical properties	Longitudinal	~ 190–245	~ 14–28	~ 1–12	~ 0.1–0.4
	Cross	~ 30–170			
Density	~ (1.5–2) $g \cdot cm^{-3}$			0.2–0.6	
Porosity	~ (3–12) %			~ 30–95	

2. Research Method

2.1. Procedure for preparation

This study used PU sponge, tapioca flour, distilled water, and AISI 316L biomaterial powder as its materials. The key ingredient in the dough used to make green bodies was AISI 316L

biomaterial, which passes through a 325 mesh screen. Twenty PPI, twenty-five PPI, thirty PPI, and thirty-five PPI were the density values for PU sponge. As a powder binder and foaming agent, tapioca flour was the preferred option.

The first step in preparing the green body was to cut the PU sponge sheet to measure 15 mm by 15 mm by 15 mm (Song et al., 2021). Figure 1 displays a digital image of a PU sponge specimen that has been created. Then, combine tapioca flour and 1% wt. distilled water to make a powder adhesive solution. Once the mixture was well combined and dissolved, it was brought to a boil.

The process of creating the AISI 316L biomaterial mixture involved mixing up to 3% of the powdered AISI 316L biomaterial by weight with a tapioca flour solution. The liquid was then blended into an AISI 316L slurry for 20 minutes at 65 rpm using a stirrer. The slurry was prepared for use in printing green bodies after being left for an hour.

By impregnating the PU sponge with AISI 316L slurry, the green body specimens are created. The sponge was immersed in slurry until it was completely covered on both the inside and outside. A green body dryer was used, and it was run for 20 minutes at 120 degrees Celsius. Retaining the slurry on the PU sponge grid is the aim of the drying process.

The Nabertherm muffle furnaces were used for the sintering process. 900, 1000, 1100, and 1200 degrees Celsius were the settings for the sintering temperature, respectively. With a holding period of 60 minutes, the heating rate was set at 200 ºC per hour. The furnace's OFF button was then turned off to complete the cooling process.

2.2. Measurements of shrinkage and porosity in porous biomaterial AISI 316L

Scanning optical microscopy was used to study the pore structure of porous AISI 316L at specific magnifications. Concurrently, the material's pore porosity is determined using the subsequent formula (Qiu et al., 2018):

$$P = 1 - \frac{P^*}{P_s} \tag{1}$$

where ρ* represents the porous density of AISI 316.

The measurement technique involves dividing the specimen's total weight by its total volume. The AISI 316L solids' density, represented by Ps, is 8.0 g/cm3. Next, using the weight of the test object both before and after sintering, the shrinkage of the object is calculated.

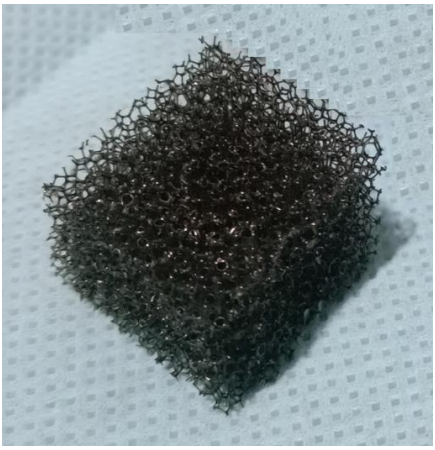

Fig 1 A digital photograph of the prepared porous material.

3. Research Results

3.1. Surface properties of the modified porous

A macrograph of the porous biomaterial AISI 316L

Results obtained from different sizes of PU sponge are displayed in Figures 2-4, which represent the macrostructure of porous 316L stainless steel. The asymmetrical pores measure roughly 0.3 mm in diameter, 0.5 mm in length, 0.7 mm in diameter, and 0.9 mm in length for PU sponges with densities of 20 PPI, 25 PPI, 30 PPI, and 35 PPI accordingly. Because part of the sample's surface is covered in 316L metal, it is not possible to see the entire distribution of pores on the sample. To ensure that the mechanical test yields reliable results, it is advised to remove the excess 316L metal that is covering the sample's exterior.

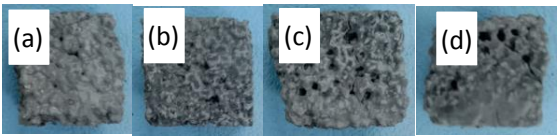

Fig 2. Macrostructure of the porous AISI 316L under a sintered of 1000 ^{o}C with different densities of PU sponge. (a) 20 PPI, (b) 25 PPI, (c) 30 PPI, and (e) 35 PPI, respectively.

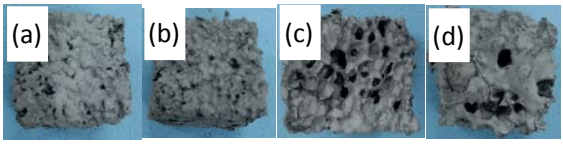

Fig 3 Macrostructure of the porous AISI 316L under a sintered of 1100 °C with different densities of PU sponge. (a) 20 PPI, (b) 25 PPI, (c) 30 PPI, and (e) 35 PPI, respectively.

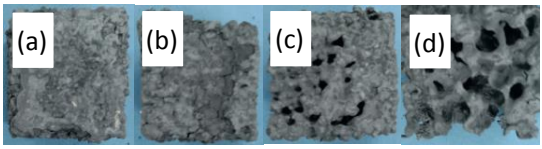

Fig 4 Macrostructure of the porous AISI 316L under a sintered of 1200 °C with different densities of PU sponge. (a) 20 PPI, (b) 25 PPI, (c) 30 PPI, and (e) 35 PPI, respectively.

A higher magnification surface macrograph of 316L stainless steel is shown in Figures 5-7. The arrows indicate that the supports are not attached, as can be seen visually. Imperfect impregnation, the slurry's adhesion force to the PU sponge material, sintering speed, sintering holding time, and cooling time can all cause the supports to separate.

The porous biomaterial AISI 316L micrograph

The micrographs of different sintering temperatures are displayed in Figure 5. The specimen exhibits weak bonding between the AISI 316 powder granules at a sintering temperature of 1000°C for all PU sponge variants. As the sintering temperature rises, these powder grains maintain their connections. Thus, strong connections exist between the grains at a sintering temperature of 1100°C. in order for the grain boundaries to become invisible. This demonstrates how the grain fragments have already merged. Finally, the pores enlarge and cover the entire surface of the material at a sintering temperature of 1200°C.

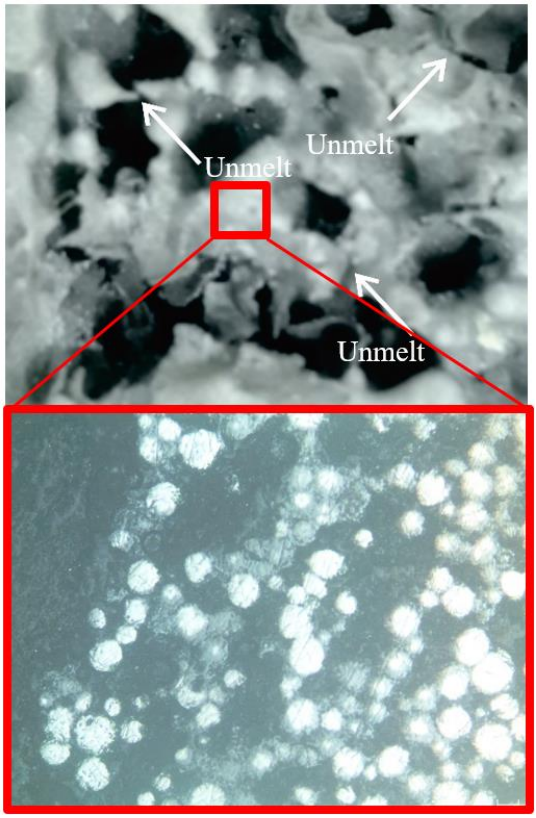

Fig 5 Microstructure of the cellular structure of the grains and sintered pore wall at 1000°C.

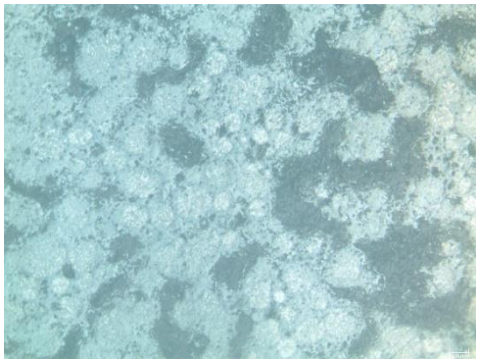

Fig 6 Microstructure of the cellular structure of the grains and sintered pore wall at 1100°C.

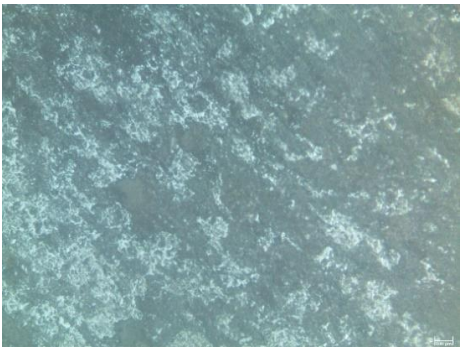

Fig 7 Microstructure of the cellular structure of the grains and sintered pore wall at 1200°C.

3.2. AISI 316L porous biomaterial's porosity and shrinkage

The percentages of porosity and mass shrinkage for porous objects containing 1% weight of sintered tapioca flour at different temperatures are displayed in Figures 8 and 9, respectively. With the exception of the sintering temperature of 1200 °C, the results indicated that shrinkage rose and porosity reduced when the sintering temperature was raised. Hu et al. (2023) found that AISI 316L holes created using tapioca starch as a space holder likewise displayed the maximum porosity value after an hour at 1200°C. The maximum porosity value was likewise seen in AISI 316L pores, which were created using tapioca starch as a space holder, after an hour at 1200°C.

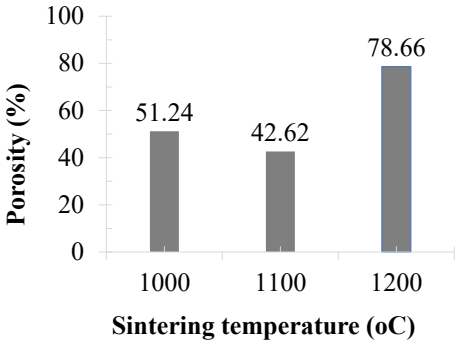

Fig 8 Porosity as a function of sintering temperature.

The shrinking process is determined by the material's inherent characteristics. An rise in sintering temperature tends to cause the specimen's pore size to decrease. Additionally, if the sintering temperature is too high, it will be destroyed. Mechanical characteristics may decrease as porosity increases (Wang et al., 2022). A sintering temperature of 1100°C resulted in the best porosity percentage of 42.62%. Observations made using an optical

microscope, as shown in Figure 6, can support this. A sintering temperature of 1200ºC, which damaged the specimen's surface, further supports these results. As seen in Figure 5, this is distinguished by the emergence of diffuse holes.

By applying a space holder technique in conjunction with a duplicate template, the highly porous AISI 316L biomaterial has been created. According to equation 1, 42.62%, or 1100 ºC, is the sintering temperature at which this porous biomaterial has the maximum porosity. According to Dewidar et al. (2007), implant materials suggested for orthopedics have porosities ranging from 20% to 59%. The findings of this study can then be suggested as an alternate material for orthopedics based on porosity.

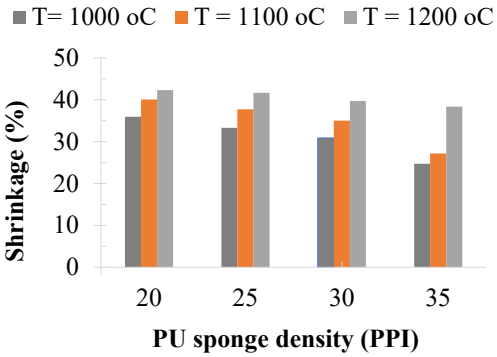

Fig 9 Shrinkage and sintering temperature of porous AISI 316L at different PU sponge densities.

4. Conclusion

This study has drawn a number of conclusions, including:

1. The space holder and replica template method can be used to create the porous AISI 316L biomaterial. PU sponge as a macropore formation medium. In addition to being a binder for AISI 316L metal powder, tapioca flour serves as a foaming agent and has the ability to produce pores—albeit tiny ones.
2. 2. PU sponge density, tapioca starch content, and sintering temperature all have significant roles in pore development. For every PU sponge density, the ideal porosity was reached at 1100 degrees Celsius. There were 42.62% micropores as a result. While porosity rises to 1200oC during sintering, cracks start to show.

Authors' Contributions

Author 1: formal analysis, conceptualization, methodology, material testing, adjustment, writing (first draft, report, review, and editing), finalization, and presentation. Conceptualization, methodology, validation, review, writing—review and editing—supervision, and accepting are the **second set of authors**. The **third author** is responsible for conceptualization, methodology, review, writing, editing, supervision, and acceptance.

Conflicts of Interest

The authors declare they have no conflicts of interest.

Acknowledgments

The writers would like to express their gratitude for being awarded the normal fundamental research grant for 2023 (contract number 005/061026/PB/SP2H/AK.04/2023). The Minister of Education, Culture, Research, and Technology of the Republic of Indonesia - Directorate General of Higher Education has our sincere gratitude. The University of Muhammadiyah Semarang Faculty of Engineering's Department of Mechanical Engineering provides support for facilities and infrastructure.

References

1. Bandyopadhyay, A., Mitra, I., Goodman, S. B., Kumar, M., & Bose, S. (2023). Improving biocompatibility for next generation of metallic implants. *Progress in Materials Science*, *133*, 101053. https://doi.org/10.1016/j.pmatsci.2022.101053

2. Čapek, J., Machová, M., Fousová, M., Kubásek, J., Vojtěch, D., Fojt, J., Jablonská, E., Lipov, J., & Ruml, T. (2016). Highly porous, low elastic modulus 316L stainless steel scaffold prepared by selective laser melting. *Materials Science and Engineering: C*, *69*, 631–639. https://doi.org/10.1016/j.msec.2016.07.027

3. Dewidar, M., Khalil, A., & Lim, J. K. (2007). Processing and mechanical properties of porous 316L stainless steel for biomedical applications. *Transactions of Nonferrous Metals Society of China*, *17*, 468–473. https://doi.org/10.1016/S1003-6326(07)60117-4

4. Du, P., Wu, Z., Li, K., Xiang, T., & Xie, G. (2021). Porous Ti-based bulk metallic glass orthopedic biomaterial with high strength and low Young's modulus produced by one step SPS. *Journal of Materials Research and Technology*, *13*, 251–259. https://doi.org/10.1016/j.jmrt.2021.04.084

5. Essa, K., Jamshidi, P., Zou, J., Attallah, M. M., & Hassanin, H. (2018). Porosity control in 316L stainless steel using cold and hot isostatic pressing. *Materials & Design*, *138*, 21–29. https://doi.org/10.1016/j.matdes.2017.10.025

6. Hu, G., Xu, G., Gao, Q., Feng, Z., Huang, P., & Zu, G. (2023). Compressive Properties and Energy Absorption Behavior of 316L Steel Foam Prepared by Space Holder Technique. *Materials*, *16*(4), Article 4. https://doi.org/10.3390/ma16041419

7. Pathote, D., Jaiswal, D., Singh, V., & Behera, C. K. (2022). Optimization of electrochemical corrosion behavior of 316L stainless steel as an effective biomaterial for orthopedic applications. *Materials Today: Proceedings*, *57*, 265–269. https://doi.org/10.1016/j.matpr.2022.02.501

8. Pathote, D., Kumari, P., Singh, V., Jaiswal, D., Gautam, R. K., & Behera, C. K. (2023). Biocompatibility evaluation, wettability, and scratch behavior of Ta-coated 316L stainless steel by DC magnetron sputtering for the orthopedic applications. *Surface and Coatings Technology*, *459*, 129392. https://doi.org/10.1016/j.surfcoat.2023.129392

9. Ravichander, B. B., Jagdale, S. H., Jabed, A., & Kumar, G. (2023). Mechanical and corrosion behavior of sheet-based 316L TPMS structures. *International Journal of Mechanical Sciences*, *254*, 108439. https://doi.org/10.1016/j.ijmecsci.2023.108439

10. Singh, P., Shrivastava, V., Abhash, A., Yadav, B. N., Singh, I. B., & Mondal, D. P. (2021). Compressive deformation and corrosion behaviour of moderate to highly porous Ti4Al4Co (wt%) alloy foam. *Materials Chemistry and Physics*, *257*, 123718. https://doi.org/10.1016/j.matchemphys.2020.123718

11. Wang, S., Yang, X., Han, Z., Wu, X., Fan, Y.-B., & Sun, L.-W. (2022). Changes of cortical bone pores structure and their effects on mechanical properties in tail-suspended rats. *Medicine in Novel Technology and Devices*, *16*, 100175. https://doi.org/10.1016/j.medntd.2022.100175.